JOC The Journal of Organic Chemistry

Article

pubs.acs.org/joc

Oligonucleotides with 1,4-Dioxane-Based Nucleotide Monomers

Andreas S. Madsen and Jesper Wengel*

Nucleic Acid Center, Department of Physics, Chemistry and Pharmacy, University of Southern Denmark, 5230 Odense M, Denmark

Supporting Information

ABSTRACT: An epimeric mixture of *H*-phosphonates **5*R*** and **5*S*** has been synthesized in three steps from known secouridine **1**. Separation of the epimers has been accomplished by RP-HPLC, allowing full characterization and incorporation of monomers **X** and **Y** into 9-mer oligonucleotides using *H*-phosphonates building blocks **5*R*** and **5*S***, respectively. A single incorporation of either monomer **X** or monomer **Y** in the central position of a DNA 9-mer results in decreased thermal affinity toward both DNA and RNA complements (ΔT_m = −3.5 °C/−3.5 °C for monomer **X** and ΔT_m = −11.0 °C/−6.5 °C for monomer **Y**). CD measurements do not reveal major rearrangements of the duplexes formed, but molecular modeling suggests that local rearrangement of the sugar phosphate backbone and decreased base interactions with neighboring bases might be the origin of the decreased stability of duplexes.

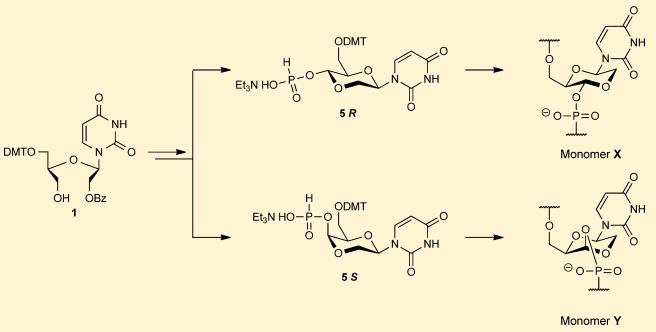

INTRODUCTION

Formal expansion of the furanose ring of nucleosides to give nucleoside analogues with six-membered rings as sugar moiety has been a significant research field during the past few decades.[1,2] Simple cyclohexane derivatives[3−5] and nucleoside analogues with 1,4-heteroatom cyclohexanes including 1,4-dioxane, 1,4-oxathiane, 1,4-dithiane, and morpholine as the sugar moiety have also been reported,[6−14] and formal 1,4-dioxane derivatives formed by hydration of 2′,3′-dialdehyde-2′,3′-*seco*-nucleosides have been reported as a stable form of such dialdehydes.[15,16] None of the above-mentioned nucleoside analogues have been incorporated into oligonucleotides (ONs) as they all, but the hydrates, lack either one or two hydroxy groups to enable phosphodiester oligomerization.

Eschenmoser initiated the field of ONs with six-membered sugar rings by the synthesis of homo-DNA and its *allo*-, *altro*- and *gluco*-pyranosyl analogues, where the furanose ring is formally expanded by a methylene (or hydroxymethylene) group between C1′ and C2′.[17] These studies demonstrated that homo-DNA:homo-DNA exhibit very strong Watson−Crick base-pairing but also reverse Hoogsteen adenine and guanine self-pairings, whereas it does not form duplexes with DNA or RNA. In a recent example, the synthesis and oligomerization of a 2′-enopyranose thymidine was realized, and interestingly, pairing with both poly(dA) and poly(rA) was demonstrated.[18]

Hexitol nucleic acid (HNA) and its hydroxylated (mannitol and altrohexitol) derivatives, formally derived from pentofuranoses by inserting a methylene group between C1′ and O4′, represents another ON system which is able to form duplexes not only with itself but also with RNA and DNA.[19−21] The hexitol skeleton mimics the C3′-*endo*-conformation adopted by RNA in RNA:RNA duplexes (stability of duplexes: HNA:HNA > HNA:RNA > HNA:DNA).[19] Furthermore, HNA has demonstrated potential as antisense drug by directing translational arrest of a targeted gene.[22]

Incorporation of nucleoside analogues with saturated and unsaturated cyclohexane rings into ONs have been realized by the formal substitution of O4′ of DNA with an ethyl or ethenyl moiety, resulting in cyclohexane nucleic acid (CNA)[23] and cyclohexene nucleic acid (CeNA),[24,25] respectively. Both form stable duplexes with RNA and DNA, and CeNA has been shown to elicit RNase H activity, although at a lower rate than phosphodiester and phosphorothioate DNA.[25] Another modification having a 6-membered ribose substitute is the so-called morpholino-NA[26] which forms neutral oligomers by linking the monomers via phosphordiamidate linkages.

Both homo-DNA and HNA are derived from RNA by formal addition of a methylene group. As hydration of duplexes plays a crucial role in duplex stability, introduction of a hydrophobic methylene moiety might not be optimal. Alternatively, the ring could be expanded by introduction of an oxygen atom. However, 1,2- and 1,3-dioxanes would be expected to be very labile, leaving only 1,4-dioxanes as potential nucleotide mimics. 1′,2′,4′- and 1′,2′,3′-substituted dioxanes (see Figure 1 for numbering)[27] bear closer resemblance to O2′-linked ribofuranosides, and 2′,3′,4′-substituted dioxanes are expected to be very unstable resulting in cleavage to the dialdehyde with the nucleobase acting as leaving group. However, 1′,3′,4′-substituted dioxanes satisfy both substitution pattern and formal resemblance to O3′-linked ribofuranosides, establishing nucleotide monomers **X** and **Y** as potential nucleotide mimics (Figure 1).

Received: January 31, 2012
Published: March 22, 2012

dx.doi.org/10.1021/jo300222q | J. Org. Chem. 2012, 77, 3878−3886

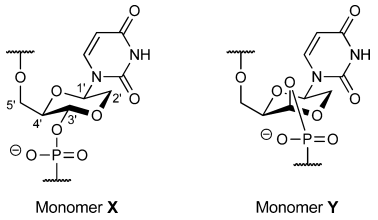

Figure 1. Structure of target monomers **X** and **Y**, with the used numbering indicated at monomer **X**.

Besides analogy with homo-DNA and HNA, monomers **X** and **Y** are appealing as they have an oxygen atom in a position expected to be close to the position of the 2′-OH group of RNA. This oxygen could potentially act as hydrogen bond acceptor, allowing preservation of structural integrity of a duplex. The corresponding free nucleotides or nucleosides could also potentially act as antiviral or anticarcinogenic drugs by offering both hydrogen bond donor and acceptor sites which could mimic the 2′- and 3′-hydroxy groups of natural nucleotides.

From a structural point of view, six-membered rings are furthermore interesting as the possible conformations and the energies needed for their interconversions are entirely different from those of the furanose ring of natural nucleotides. Thus, whereas the furanose ring of natural nucleotides has a relatively low energy barrier for the pseudorotation between *N*-type and *S*-type conformers ($\Delta G^{\ddagger}_{c}$ = 8−20 kJ/mol),[28,29] inversion between the two chair conformations of both unsubstituted cyclohexane and 1,4-dioxane is found to proceed through several higher energy transition states and metastable intermediates ($\Delta G^{\ddagger}_{c}$ = 40 kJ/mol).[30−33] As a result, 1,4-dioxane nucleotides are expected to show a smaller conformational freedom than natural furanose nucleotides.

With the above-mentioned considerations in mind, we therefore set to synthesize oligonucleotides containing monomers **X** and **Y**.

RESULTS AND DISCUSSION

Synthesis of Hemiacetal 3. Hemiacetal **3**, expected to exist as an equilibrium between its two epimeric forms, was identified as key intermediate from which both monomers **X** and **Y** could conceivably be obtained. As selective O2′-benzoylation of the corresponding 2′,3′-diol to give benzoate ester **1** has recently been described en route to UNA (unlocked nucleic acid),[34] a synthetic scheme of oxidation of the free 3′-hydroxy group of alcohol **1** followed by O2′-debenzoylation was preferred over routes including either 3′-selective oxidation of the 2′,3′-diol or 2′-selective reduction of the corresponding 2′,3′-dialdehyde.

Of the many possible oxidation methods known, acidic methods such as Swern or chromium-based oxidations were unfeasible (leading to rapid cleavage of the trityl ether, giving two primary hydroxy groups, distinguishable only by the prochirality of the *β*-position (i.e., C4′)). Nonacidic DMSO-based oxidations as Pfitzner−Moffatt and Parikh−Döering oxidation proved unsuccessful, as did the otherwise widespread Dess−Martin periodinane oxidation. However, oxidation was readily effected by IBX (*o*-iodoxybenzoic acid) in pyridine/EtOAc at near-reflux.[35,36] By NMR spectroscopy, oxidation to give aldehyde **2** was confirmed by the disappearance of signals corresponding to H3′ and 3′-OH and the appearance of a peak at 9.75 ppm (^{1}H NMR), and by a downfield shift to 200.3 ppm of the peak corresponding to C3′ (^{13}C NMR). Despite the extremely easy workup for this reaction, varying amounts of the corresponding hydrate could be detected in all reaction mixtures isolated and analyzed. As a result, oxidation followed by debenzoylation by sodium hydroxide in methanol was carried out as a two step procedure without purification of the aldehyde intermediate, affording hemiacetal **3*R*/*S*** in an approximate 1:1 ratio (according to ^{1}H NMR) in 67% yield over two steps (Scheme 1). Disappearance of the signal from the aldehyde moiety in ^{1}H NMR upon cleavage of the benzoyl ester indicates ring closure to the hemiacetal, with no detectable presence of the hydroxyaldehyde.

Phosphoramidite Strategy. The epimeric mixture of hemiacetal **3*R*/*S*** reacted readily with 2-cyanoethyl *N*,*N*-diisopropylphosphoramidochlorodite in CH_2Cl_2 resulting in four diastereoisomers in 73% combined yield (Scheme 1). Even though C3′ is the most relevant stereocenter—as the phosphorus atom of the resulting phosphodiesters after oligonucleotide synthesis is nonchiral—full separation and assignment of configuration at the two stereocenters was desired for all four diastereomers, especially as we wanted to obtain oligonucleotides containing monomers **X** and **Y** with defined C3′ configuration. However, only partial separation of the four diastereoisomers could be accomplished by silica gel column chromatography. The mixture could be separated into two fractions, each containing two phosphoramidites (^{31}P NMR (121 MHz, $CDCl_3$) *δ* 149.5 ppm and 150.1 ppm (∼1:4 ratio, termed **4A**/**B**) and 152.0 ppm and 152.4 ppm (∼6:1 ratio, termed **4C**/**D**), respectively). Attempts to separate the binary mixtures by RP-HPLC were also unsuccessful, giving only partial separation even on analytical (1.0 mg) scale. As a result of the poor resolution obtained, in combination with the risk of degradation of the phosphoramidites during workup, separation of phosphoramidites **4** was not pursued further.

Scheme 1. Synthesis of Phosphoramidites 4 and *H*-Phosphonates 5

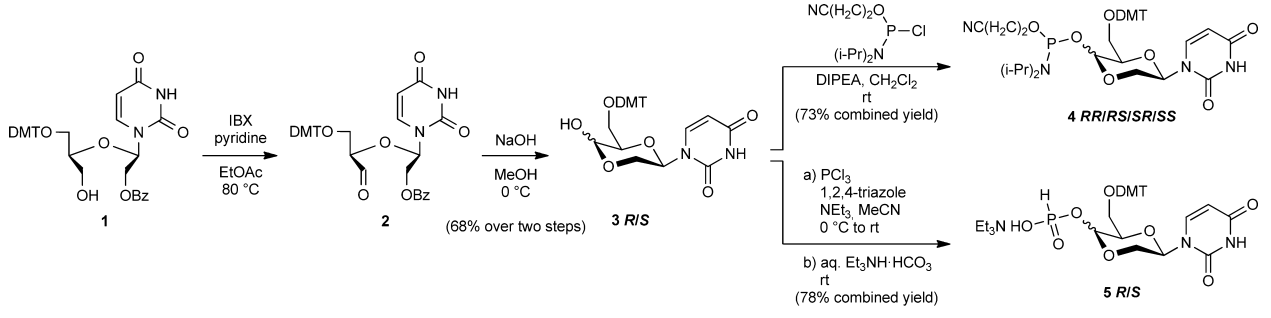

dx.doi.org/10.1021/jo300222q | J. Org. Chem. 2012, 77, 3878−3886

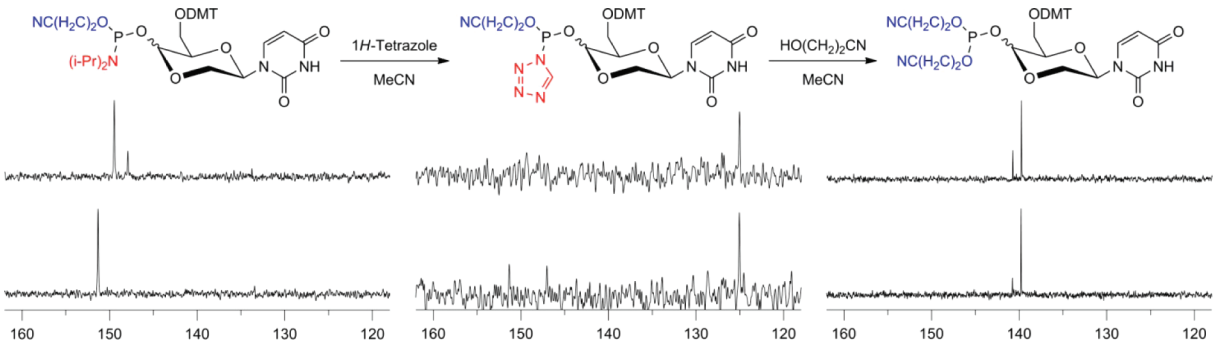

Figure 2. ^{31}P NMR spectra after coupling of phosphoramidite mixtures **4A**/**B** and **4C**/**D** (top and bottom, respectively) with 2-cyanoethanol, demonstrating that both binary mixtures contain both C3′-epimers. Spectra of amidites and activated amidites are recorded at 81 MHz. Spectra of final phosphites are recorded at 121 MHz.

Direct assignment of stereochemistry at C3′ (and at the chiral phosphorus atom) of the two components of the binary mixtures of phosphoramidites **4** was not feasible by ^{1}H NMR due to the complexity of the spectra and the low intensity of the minor isomer. As an alternative to full separation and configurational assignment, the relative C3′ stereochemistry of the binary mixtures was determined. Each of the separated binary mixtures was coupled with 3-hydroxypropionitrile (2-cyanoethanol) in dry acetonitrile, using 1*H*-tetrazole as activator, and the progress of the reactions was monitored by ^{31}P NMR (see Figure 2). The phosphorus atom of the resulting phosphite triesters is not stereogenic, thereby allowing relative assignment of C3′ stereochemistry of the four phosphoramidites. After the phosphoramidites were stirred with 1*H*-tetrazole for 60 min, a ^{31}P NMR spectrum showed a single peak at 125.1 ppm. The single peak observed is in agreement with previous reports on activation of phosphoramidites, probably as a result of epimerization of phosphorus via exchange with excess tetrazole.[37] The very long activation time was needed to convert all starting material to the activated tetrazolide as indicated by ^{31}P NMR. While the need for shorter reaction times has been reported for simultaneous activation and coupling,[38] i.e., mixing phosphoramidite, tetrazole, and alcohol, the long reaction time needed in our investigation is likely a consequence of the sequential approach used, leading to slower kinetics in the activation step. Subsequently, excess anhydrous 2-cyanoethanol was added, and the reaction mixture was stirred until ^{31}P NMR indicated full conversion of the tetrazolide to the corresponding phosphite triesters. Both binary mixtures, however, give rise to spectra having *two* peaks, an intensive peak at 139.8 ppm and a less intensive peak at 140.8 ppm. Thus, both binary mixtures consist of two diastereomers having alternate C3′ stereochemistry. Direct incorporation of the two binary mixtures into oligonucleotides would therefore yield an undesirable mixture of two diastereomeric ONs (containing either monomer **X** or **Y**), and as a result ON synthesis using this strategy was not pursued.

***H*-Phosphonate Strategy.** One of the drawbacks of the phosphoramidite strategy is, as described above, the formation of two stereogenic centers upon phosphitylation of hemiacetal **3**, thereby adding complexity to the following separation step. Phosphoramidite chemistry is usually the method of choice in ON synthesis, due to commercial availability of standard monomer building blocks and well-established automated solid-phase synthetic protocols.[39−42] However, phosphotriester and *H*-phosphonate methodologies have also been successfully employed.[43] *H*-Phosphonate building blocks for natural nucleosides are commercially available, and the corresponding solid phase ON synthetic protocols are well established with coupling yields comparable to those obtained with phosphoramidite building blocks.[44] An appealing feature of the *H*-phosphonate approach is the nonstereogenic nature of the *H*-phosphonate moiety of the monoester building blocks, whereby the major obstacle in the phosphoramidite strategy could be circumvented. Furthermore, several examples of phosphorylation via *H*-phosphonates on epimeric positions have been reported in the literature.[45−48]

Gratifyingly, *H*-phosphonates **5*R*/*S*** were easily obtained by treating hemiacetal **3** with PCl_3/1,2,4-triazole followed by hydrolysis, resulting in an epimeric mixture of *H*-phosphonates **5*R*/*S*** in an approximate 1:1 ratio (according to ^{1}H NMR) in 78% yield. Attempts to separate epimers **5*R*/*S*** by silica gel column chromatography were unsuccessful; however, separation could be realized by RP-HPLC on both small scale (~50 μg) and a more practical scale (6−10 mg). A representative RP-HPLC profile with retention times of 43.9 min (faster eluding compound) and 45.8 min (slower eluding compound) is shown in Figure 3. Subsequently, appropriate fractions were pooled,

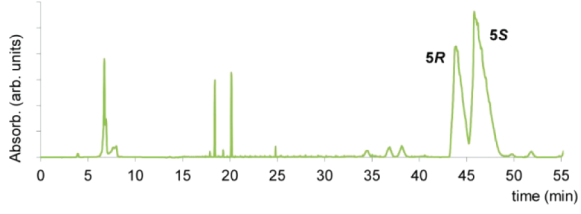

Figure 3. Representative RP-HPLC profile for the separation of *H*-phosphonate epimers **5*R*/*S***.

concentrated under reduced pressure, and then lyophilized to afford the two separated epimers as white foams. This procedure allowed isolation of enough material to realize full characterization and individual incorporation of epimers **5*R*** and **5*S*** into ONs.

Assignment of 3′-Stereochemistry of *H*-Phosphonates 5. Several factors, including intramolecular steric and electronic factors as well as solvation, contribute to the free energy of the conformations of *H*-phosphonates **5*R*** and **5*S***. However, the dioxane ring would be expected to adopt a chair conformation where two conformations of the dioxane ring are possible for each of the epimers. This is in agreement with the observed conformation of closely related (2*R*,6*R*)-6-hydrox-

dx.doi.org/10.1021/jo300222q | *J. Org. Chem.* 2012, 77, 3878−3886

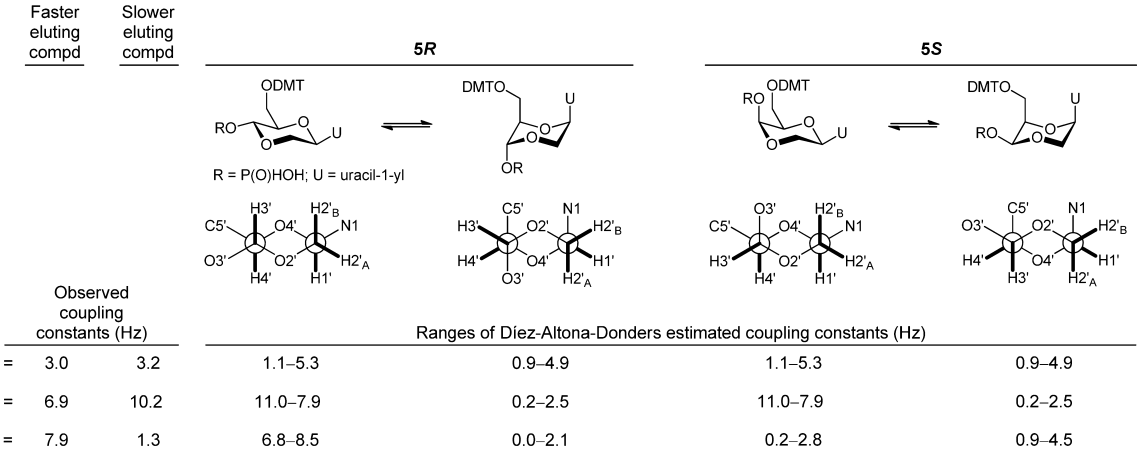

Figure 4. Two possible conformations of *H*-phosphonate **5*R*** and **5*S***, respectively, including the corresponding double-barreled Lewis structures, and observed and estimated coupling constants.

Table 1. Thermal Denaturation Studies of Matched and Mismatched Duplexes[a]

	T_m [ΔT_m/mod] (°C)							
	DNA: 3′-CAC TBT ACG				RNA: 3′-CAC UBU ACG			
B =	A (**ON4**)	C (**ON5**)	G (**ON6**)	T (**ON7**)	A (**ON8**)	C (**ON9**)	G (**ON10**)	U (**ON11**)
5′-GTG ATA TGC (**ON1**)	29.0	13.0 [−16.0]	20.0 [−9.0]	14.0 [−15.0]	27.0	<10 [<−17.0]	24.0 [−3.0]	<10 [<−17.0]
5′-GTG AXA TGC (**ON2**)	25.5 [−3.5]	14.0 [−11.5]	20.5 [−5.0]	18.5 [−7.0]	23.5 [−3.5]	<10 [<−13.5]	*b*	13.5 [−10.0]
5′-GTG AYA TGC (**ON3**)	18.0 [−11.0]	<10 [<−8.0]	<10 [<−8.0]	17.0 [−1.0]	20.5 [−6.5]	<10 [<−10.5]	12.0 [−8.5]	<10 [<−10.5]

[a]Thermal denaturation temperatures of **ON2** and **ON3** toward DNA or RNA complements (**ON4** and **ON8**, respectively) [T_m values/°C (ΔT_m = change in T_m value, for matched duplexes calculated relative to **ON1**:**ON4** or **ON1**:**ON8**, for mismatched duplexes calculated relative to matched duplex)] measured as the maximum of the first derivative of the melting curve (A_{260} vs temperature) recorded in medium salt buffer ([Na^+] = 110 mM, [Cl^-] = 100 mM, pH 7.0 (NaH_2PO_4/Na_2HPO_4)), using 1.0 μM concentrations of the two ONs. T_m values are averages of at least two measurements. [b]Broad transition.

ymethyl-2-(uracil-1-yl)-1,4-dioxane,[13] where the 1,4-dioxane ring adopts a chair conformation with uracil and hydroxymethyl in equatorial positions, despite the potential stabilization of the nucleobase adopting an axial conformation by the anomeric effect. The size of the nucleobase and hydroxymethyl moieties most probably lead to significant 1,3-diaxial interactions, thereby destabilizing the diaxial conformation. These observations strongly suggest that the N1−C1′−O4′−C4′−C5′ part of *H*-phosphonates **5*R*/*S*** will induce a similar conformation with the nucleobase and the 4′-substituent in equatorial positions, whereas the anomeric effect of O3′ would be expected to stabilize an axial position of the O3′-phosphonate functionality.

To determine the C3′-configuration of the separated *H*-phosphonates, the coupling constants (*J* values) observed in ^{1}H NMR of the separated *H*-phosphonates were investigated and compared to values predicted by the Díez−Altona−Donders equation[49] as incorporated in the MestRe-J program[50] (see Figure 4). $J_{1',2'A}$, $J_{1',2'B}$, and $J_{3',4'}$ are all correlated to dioxane conformation, and naturally, $J_{3',4'}$ is correlated with C3′-configuration. Importantly, only the N1,C5′-equatorial/O3′-axial conformation of *H*-phosphonate **5*S*** is predicted to have $J_{1',2'B}$ and $J_{3',4'}$ matching the 10.2 and 1.3 Hz, respectively, observed for the slower eluting epimer. As a consequence, the faster eluting epimer must be *H*-phosphonate **5*R*** and gratifyingly the N1,O3′,C5′ equatorial conformation of this is the only conformation predicted to have a $J_{3',4'}$ matching the 7.9 Hz observed for the fast eluting epimer.

ON Synthesis Using *H*-Phosphonates 5*R* and 5*S*. For homo-DNA, data solely exist for fully modified ONs, whereas a few HNA−DNA hybrids have been synthesized.[19,22] Evaluation of fully or multiply modified ONs of either of the dioxane monomers introduced herein would be very interesting as they could further improve the knowledge about six-membered nucleotide mimics and elucidate if a continuous stretch of dioxane monomers could lead to favorable backbone geometry. However, such evaluation requires future development of improved synthetic and separation procedures, and since a preliminary evaluation of binding affinity can be accomplished with only one incorporation, we decided not to pursue multiple incorporations of monomers **X** and **Y**. Singly modified polyT oligomers (e.g., dT_6XdT_6), as reported for HNA,[19] could possibly be synthesized, thereby allowing direct comparison, but analysis of such duplexes is hampered by the possibility of both parallel and antiparallel binding to a complement ON, and we therefore chose to evaluate monomers **X** and **Y** as single incorporations in a mixed sequence.

ON2 and **ON3** containing a single central incorporation of monomer **X** or **Y**, respectively, were synthesized by manual solid support synthesis using the synthetic cycle outlined in the Experimental Section. Coupling yields of *H*-phosphonates **5*R*** and **5*S*** were 69% and 76%, respectively, according to the absorbance measured after detritylation, whereas standard nucleoside *H*-phosphonates coupled in >95% stepwise yields. The synthesized oligonucleotides were purified by RP-HPLC,

dx.doi.org/10.1021/jo300222q | J. Org. Chem. 2012, 77, 3878−3886

and their constitution and purity (>80%) was verified by MALDI-MS analysis and ion-exchange-HPLC, respectively. **ON2** (monomer **X**) and **ON3** (monomer **Y**) were both obtained in ~15% overall yield as estimated from UV measurements and loading of the synthesis support used. The aqueous stability of the synthesized ONs was tested by a sample stored at rt for two weeks. Both unmodified (**ON1**) and modified ONs (**ON2** and **ON3**) proved stable under these conditions with no observable cleavage as evaluated by IC-HPLC (see Figure S1, Supporting Information).

Thermal Denaturation and Circular Dichroism Experiments. The influence on thermal stability of DNA:DNA and DNA:RNA duplexes of a single incorporation of either monomers **X** and **Y** was evaluated by UV−thermal duplex denaturation studies (Table 1). Unless otherwise noted, the UV−thermal denaturation curves displayed smooth sigmoidal monophasic transitions similar to the unmodified reference duplexes.

Incorporation of a single monomer **X** resulted in a slight decrease in thermal affinity toward DNA and RNA complements when compared to unmodified DNA (ΔT_m = −3.5 °C against both DNA and RNA), whereas single incorporation of monomer **Y** resulted in a dramatic decrease in thermal affinity toward a DNA complement (ΔT_m = −11.0 °C) and a substantial but less dramatic decrease in thermal affinity toward an RNA complement (ΔT_m = −6.5 °C). To investigate if the uracil moiety of monomers **X** and **Y** forms hydrogen bonding with an opposing complementary adenosine monomer, thermal denaturation studies were carried out toward DNA and RNA strands with an opposing mismatched nucleotide. For monomer **X**, mismatch discrimination was observed for all mismatches both against DNA and RNA, except for U:rG, where a very broad transition did not allow determination of T_m. For monomer **Y** good to excellent mismatch discrimination was observed, except for the U:T mismatch.

Although the thermal stabilities are significantly different, CD curves of **ON1**, **ON2**, and **ON3** in duplexes with complementary DNA (**ON4**) are nearly identical (see Figure 5a). All three curves display distinctive B-type DNA signatures, including a positive peak at 280 nm and a negative peak at 250 nm. For duplexes formed with complementary RNA (**ON8**), the overall features of the curves are identical, even though the negative peaks observed in the spectrum of **ON1**:**ON8** at 210 and 240 nm are less prominent for **ON2**:**ON8** and even positive (though still distinctive local minima) for **ON3**:**ON8** (see Figure 5a). Consequently, duplex **ON2**:**ON8** must be very similar to the A/B-duplex type of DNA:RNA, whereas **ON3**:**ON8** attains a slightly different duplex type. However, the CD spectra do not hint at the origin of the reduced thermal affinity of **ON2** and **ON3** toward complements.

Molecular Modeling of Duplexes ON2:DNA and ON3:DNA. To rationalize the observed decreased thermal affinities of **ON2** and **ON3** toward their DNA complement, the behavior of monomers **X** and **Y** in DNA:DNA duplexes was evaluated by molecular modeling of duplexes **ON1**:**ON4**, **ON2**:**ON4**, and **ON3**:**ON4**. As CD curves indicated that the overall duplex geometry was not changed upon incorporation of the modified monomers, a standard B-type DNA duplex was modified in MacroModel v9.1[51] to give the duplexes of interest. The model structures were subjected to a 5 ns stochastic dynamics simulation, using the amber94 force field[52] with the improved parambsc0 parameters[53] incorporated and GB/SA solvation model[54] in MacroModel V9.1.[51] However, the optimized parameters do not take modified nucleotides into account, and the original amber94 parameters were therefore used for monomers **X** and **Y** and the 3′-neighboring nucleotide. During simulation, structures were collected at evenly distributed intervals to allow conformational analysis during the simulation trajectory.

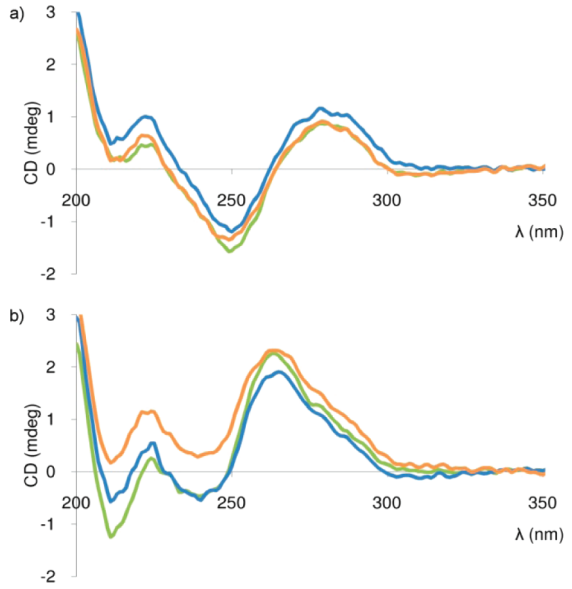

Figure 5. Circular dichroism spectra: (a) **ON1**:**ON4** (green), **ON2**:**ON4** (blue), **ON3**:**ON4** (orange); (b) **ON1**:**ON8** (green), **ON2**:**ON8** (blue), **ON3**:**ON8** (orange). The spectra were recorded at 5 °C otherwise using the same experimental conditions as for thermal denaturation experiments.

The altered sugar moiety of dioxane nucleotides **X** and **Y** precludes direct conformational comparison with unmodified DNA; however, some qualitative considerations can be made by comparison of the two modified monomers. Furthermore, overall nucleotide parameters (e.g., intrastrand phosphate distance (P_n to P_{n+1})) can evaluate the fit of the modified nucleotides in a duplex context. The duplex conformations obtained from the modeling trajectory demonstrate that monomer **Y** is present in an almost ideal chair conformation ($^{C3'}C_{C1'}$), whereas monomer **X** needs to adopt a boat conformation ($B_{O2',O4'}$) to allow accommodation in the duplex structure (see Figure 6).

As might be expected, the chair conformation of monomer **Y** explores a much smaller fraction of the conformational space than the energetically less favored twist boat conformation of monomer **X**. However, neither of the monomers displays radical conformational changes (e.g., shifts from $^{C3'}C_{C1'}$ to

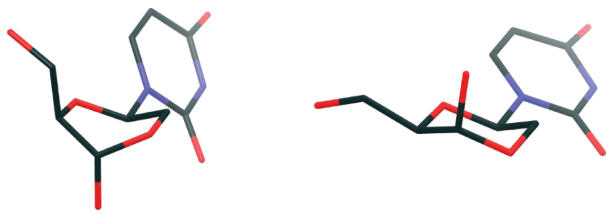

Figure 6. Close up of monomers **X** (left) or **Y** (right) as incorporated in energy-minimized duplexes, displaying $B_{O2',O4'}$ and $^{C3'}C_{C1'}$ conformations, respectively.

dx.doi.org/10.1021/jo300222q | J. Org. Chem. 2012, 77, 3878−3886

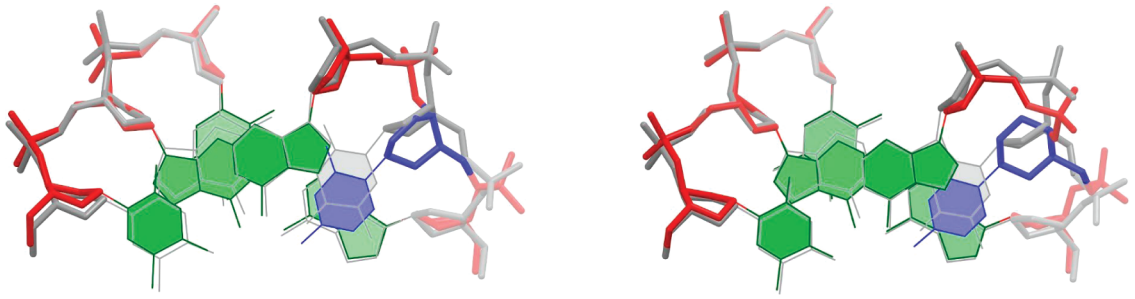

Figure 7. Truncated structures of energy-minimized duplexes with incorporation of monomers **X** (left) or **Y** (right) demonstrating a shift of the nucleobase into the major groove. Overlay in gray is the unmodified DNA:DNA duplex.

$^{C1'}C_{C3'}$). Furthermore, both dioxane monomers display a longer and much narrower distribution of the P_n-P_{n+1} distance (6.8 Å, ±0.2 Å for both monomers) than found in the unmodified DNA:DNA duplex (5.0 Å, ±0.6 Å). For monomer **X**, the longer P−P distance is accompanied by a shift of the 3′-phosphate group into the minor groove indicating the need for major alterations of the backbone to accommodate the dioxane nucleotide. Furthermore, the nucleobase is shifted approximately 1.1 Å into the major groove compared to the unmodified reference duplex, thereby significantly decreasing stacking with $\mathbf{A}_4$ (the 5′-neighbor, see Figure 7).

Almost the same shift of the nucleobase is seen for monomer **Y** (∼0.9 Å), and rearrangement of the phosphate backbone is also observed, indicating a major rearrangement of the backbone to accommodate the dioxane moiety. As a result of the rearrangement, the 3′-phosphate group is perturbed into the major groove compared to the unmodified reference duplex. Neighboring nucleotides display an increased *S*-type conformation for both the 5′- and the 3′-neighbor of monomer **X** ($N/S(\mathbf{A}_4)$ = 1%/96% and $N/S(\mathbf{A}_6)$ = 2%/92%, compared to $N/S(\mathbf{A}_4)$ = 4%/74% and $N/S(\mathbf{A}_6)$ = 4%/81% for the unmodified duplex). On the contrary, no indication of conformational tuning for monomer **Y** is found. Conformational tuning of neighboring nucleotides by LNA monomers is well established[55−57] and likely to contribute to the observed increased thermal stability of LNA duplexes. Likewise, the conformational tuning effect of monomer **X** may influence the thermal stability of the duplexes, and is possibly a contributing factor to the difference between the destabilizing effects of monomers **X** and **Y**.

Displacement of phosphate groups into the grooves could potentially disrupt the structural water surrounding the duplex, leading to a destabilization of the structure. Likewise is the shift of the nucleobase a likely origin of destabilization by decreased stacking interactions and larger exposed hydrophobic surface. For monomer **X**, the adopted boat conformation is expected to be energetically unfavorable, which most likely contributes significantly to the destabilization of the corresponding duplex. However, the molecular modeling structures do not provide an obvious explanation for the difference in thermal affinity induced by the two modified duplexes, but the combination of unfavorable conformations and low flexibility would be expected to decrease the possibility of accommodating the modified monomers in the duplex structure, leading in general to the observed low stability structures.

■ CONCLUSION

H-Phosphonates **5R** and **5S** were synthesized as an epimeric mixture in 53% yield over three steps from known secouridine **1**. Crucially, separation of the epimeric mixture by HPLC allowed full characterization of the individual *H*-phosphonates and individual incorporation of monomers **X** and **Y** into oligonucleotides. These are the first examples of the use of dioxane as sugar moiety in oligonucleotides. Thermal denaturation and circular dichroism measurements demonstrate that deoxyoligonucleotides containing a single incorporation of either monomer are capable of duplex formation with both DNA and RNA complements. Furthermore, Watson Crick base pairing capability is retained, despite a decrease of T_m of the formed duplex. Overall the results indicate that the 1,4-dioxane skeleton of monomers **X** and **Y** are nonideal mimics of the natural furanose moiety of DNA and RNA.

■ EXPERIMENTAL SECTION

(2*R*/*S*,3*R*,5*R*)-3-(4,4′-Dimethoxytrityloxymethyl)-2-hydroxy-5-(uracil-1-yl)-1,4-dioxane (3*R*/*S*). IBX (*o*-iodoxybenzoic acid, 3.04 g, 10.9 mmol) was suspended in anhydrous EtOAc (150 mL) and pyridine (1.10 mL, 13.6 mmol), and the resulting suspension was heated under stirring to 80 °C. Alcohol **1** (3.54 g, 5.43 mmol) was dissolved in anhydrous EtOAc (50 mL) and added to the heated suspension. After being stirred at 80 °C for 5 h, the suspension was cooled to 0 °C, and the precipitate was filtered off and washed with cold EtOAc (2 × 25 mL). The combined organic phase was evaporated to dryness under reduced pressure to afford a white foam, tentatively assigned as aldehyde **2** [TLC (5% EtOH in CH_2Cl_2): R_f(**1**) = 0.3, R_f(**2**) = 0.35; ^{1}H NMR (DMSO-d_6) δ 11.43 (d, $J_{NH,5}$ = 2.2, 1H, NH), 9.56 (s, 1H, CHO), 7.91−7.98 (m, 2H, $H2_{Bz}$,$H6_{Bz}$), 7.75 (d, $J_{6,5}$ = 8.0, 1H, H6), 7.65−7.72 (m, 1H, $H4_{Bz}$), 7.50−7.57 (m, 2H, $H3_{Bz}$,$H5_{Bz}$), 7.15−7.34 (m, 9H, $H2_{DMT}$, $H6_{DMT}$, $H2'_{DMT}$, $H6'_{DMT}$, $2''_{DMT}$, $H3''_{DMT}$, $H4''_{DMT}$, $H5''_{DMT}$, $H6''_{DMT}$), 6.83−6.88 (m, 4H, $H3_{DMT}$, $H5_{DMT}$, $H3'_{DMT}$, $H5'_{DMT}$), 6.13 ($dd_{ABX,X}$, $J_{1',2'B}$ = 6.1, $J_{1',2'A}$ = 5.4, 1H, H1′), 5.61 (dd, $J_{5,6}$ = 8.0, $J_{5,NH}$ = 2.2, 1H, H5), 4.74−4.82 ($m_{ABX,A}$, $J_{2'A,2'B}$ = 11.7, $J_{2'A,1'}$ = 5.4, 1H, $H2'_A$), 4.60−4.68 ($m_{ABX,B}$, $J_{2'B,2'A}$ = 11.7, $J_{2'B,1'}$ = 6.1, 1H, $H2'_B$), 4.42 (dd, $J_{4',5'A}$ = 5.4, $J_{4',5'B}$ = 3.0, 1H, H4′), 3.72 (s, 6H, OCH_3), 3.22−3.34 (m, 2H, H5′), traces of EtOAc was detected; ^{13}C NMR (DMSO-d_6) δ 200.3 (CHO), 164.9 (COPh), 162.9 (C4), 158.0 ($C4_{DMT}$,$C4'_{DMT}$), 151.0 (C2), 144.4 ($C1''_{DMT}$), 140.2 (C6), 135.1 ($C1_{DMT}$/$C1'_{DMT}$), 135.0 ($C1_{DMT}$/$C1'_{DMT}$), 133.7 ($C4_{Bz}$), 129.6 ($C2_{DMT}$, $C6_{DMT}$, $C2'_{DMT}$, $C6'_{DMT}$), 129.2 ($C2_{Bz}$, $C6_{Bz}$/$C3_{Bz}$, $C5_{Bz}$), 129.0 ($C1_{Bz}$), 128.8 ($C2_{Bz}$, $C6_{Bz}$/$C3_{Bz}$, $C5_{Bz}$), 127.8 ($C2''_{DMT}$, $C6''_{DMT}$/$C3''_{DMT}$, $C5''_{DMT}$), 127.6 ($C2''_{DMT}$, $C6''_{DMT}$/$C3''_{DMT}$, $C5''_{DMT}$), 126.7 ($C4''_{DMT}$), 113.2 ($C3_{DMT}$, $C5_{DMT}$, $C3'_{DMT}$, $C5'_{DMT}$), 102.3 (C5), 85.6 (CAr_3), 82.1 (C1′/C4′), 81.2 (C1′/C4′), 63.2 (C2′/C5′), 62.1 (C2′/C5′), 54.9 (OCH_3) ppm; ESI-HiRes *m*/*z* 673.2132 ($[M + Na]^+$, $C_{37}H_{34}N_2O_9Na^+$ calcd 673.2157)]. The resulting crude aldehyde **2** was dissolved in anhydrous MeOH (10 mL) and added to a solution of NaOH (1.30 g, 32.5 mmol) in anhydrous MeOH (200 mL). The resulting mixture was stirred under Ar at 0 °C. After the mixture was stirred for 70 min, satd aq NH_4Cl (50 mL) was added, and the resulting mixture was stirred for 10 min. Brine (50 mL) was added, and extraction with CH_2Cl_2 (3 × 200 mL) was performed. The combined organic phase was evaporated to dryness under reduced

dx.doi.org/10.1021/jo300222q | J. Org. Chem. 2012, 77, 3878−3886

pressure, and the resulting residue was purified by silica gel column chromatography (30−60% EtOAc in toluene) to afford an epimeric mixture of hemiacetal **3** (2.03 g, 68% from **1**) as a white solid: TLC (10% MeOH in CH_2Cl_2) R_f = 0.3; ^{1}H NMR (DMSO-d_6) δ 11.48 (d, $J_{NH,5}$ = 2.0, 1H, ex, NH_R/NH_S), 11.46 (d, $J_{NH,5}$ = 2.1, 1H, ex, NH_R/NH_S), 7.74 (d, $J_{6,5}$ = 8.1, 1H, $H6_S$), 7.64 (d, $J_{6,5}$ = 8.1, 1H, $H6_R$), 7.36−7.45 (m, 4H, $H2''_{DMT}$, $H6''_{DMT}$), 7.18−7.33 (m, 14H, $H4''_{DMT}$, $H2_{DMT}$, $H6_{DMT}$, $H2'_{DMT}$, $H6'_{DMT}$, $H2''_{DMT}$, $H6''_{DMT}$), 6.99 (d, $J_{OH,3'}$ = 6.8, 1H, ex, 3′-OH_S), 6.84−6.90 (m, 8H, $H3_{DMT}$, $H5_{DMT}$, $H3'_{DMT}$, $H5'_{DMT}$), 6.69 (d, $J_{OH,3'}$ = 6.5, 1H, ex, 3′-OH_R), 5.68−5.78 (m, 4H, $H1'_S$, $H1'_R$, $H5_S$, $H5_R$), 4.85 (dd, $J_{3',OH}$ = 6.5, $J_{3',4'}$ = 1.9, 1H, $H3'_R$), 4.77 (dd, $J_{3',4'}$ = 8.0, $J_{3',OH}$ = 6.7, 1H, $H3'_S$), 4.10−4.16 (m, 1H, $H4'_R$), 3.65−3.93 (m, 16H, 3 × $H2'_S/H2'_R$, $H4'_S$, $OCH_{3,S}$, $OCH_{3,R}$), 3.48−3.57 (m, 1H, $H2'_S/H2'_R$), 3.05−3.19 (m, 3H, 2 × $H5'_S$, $H5'_R$), 2.96−3.03 (m, 1H, $H5'_R$) ppm;[56] ^{13}C NMR (DMSO-d_6) δ 163.0 ($C4_R/C4_S$), 162.9 ($C4_R/C4_S$), 158.08 ($C4_{DMT,R}$, $C4'_{DMT,R}/C4_{DMT,S}$, $C4'_{DMT,S}$), 158.05 ($C4_{DMT,R}$, $C4'_{DMT,R}/C4_{DMT,S}$, $C4'_{DMT,S}$), 150.1 ($C2_R/C2_S$), 150.0 ($C2_R/C2_S$), 144.84 ($C1''_{DMT,R}/C1''_{DMT,S}$), 144.76 ($C1''_{DMT,R}/C1''_{DMT,S}$), 140.5 ($C6_R/C6_S$), 140.4 ($C6_R/C6_S$), 135.6 ($C1_{DMT,R}$, $C1'_{DMT,R}/C1_{DMT,S}$, $C1'_{DMT,S}$), 135.4 ($C1_{DMT,R}$, $C1'_{DMT,R}/C1_{DMT,S}$, $C1'_{DMT,S}$), 129.8 ($C2_{DMT}$, $C6_{DMT}$, $C2'_{DMT}$, $C6'_{DMT}$), 127.8 ($C2''_{DMT}$, $C3''_{DMT}$, $C5''_{DMT}$, $C6''_{DMT}$), 126.7 ($C4''_{DMT}$), 113.1 ($C3_{DMT}$, $C5_{DMT}$, $C3'_{DMT}$, $C5'_{DMT}$), 102.1 ($C5_S/C5_R$), 102.0 ($C5_S/C5_R$), 91.8 ($C3'_S$), 87.1 ($C3'_R$), 85.5 ($CAr_{3,R}/CAr_{3,S}$), 85.3 ($CAr_{3,R}/CAr_{3,S}$), 78.7 ($C4'_S$), 77.9 ($C1'_S/C1'_R$), 77.50 ($C4'_R/C1'_S/C1'_R$), 77.45 ($C4'_R/C1'_S/C1'_R$), 64.8 ($C2'_S/C2'_R$), 63.0 ($C5'_S/C5'_R$), 62.9 ($C5'_S/C5'_R$), 58.6 ($C2'_S/C2'_R$), 55.0 (OCH_3) ppm; ESI-HiRes *m/z* 569.1898 ([M + Na]$^+$, $C_{30}H_{30}N_2O_8Na^+$ calcd 569.1894).

(2*R*/*S*,3*R*,5*R*,P*R*/*S*)-2-Cyanoethoxy(diisopropylamino)-phosphinoxy-3-(4,4′-dimethoxytrityloxymethyl)-5-(uracil-1-yl)-1,4-dioxane (4*RR*/*RS*/*SR*/*SS*). An epimeric mixture of hemiacetal **3** (510 mg, 0.933 mmol) was coevaporated with 1,2-dichloroethane (2 × 3 mL) and redissolved in anhydrous CH_2Cl_2 (5.0 mL), and anhydrous DIPEA (1.0 mL) was added at rt, followed by dropwise addition of 2-cyanoethyl *N*,*N*′-(diisopropyl)phosphoramidochloridite (0.31 μL, 1.37 mmol). The reaction mixture was stirred at rt for 65 min, EtOH (2 mL) was added, and stirring was continued at rt for 20 min. The reaction mixture was poured into CH_2Cl_2 (20 mL) and washed with satd aq $NaHCO_3$ (10 mL) and brine (10 mL). The combined aqueous phase was back-extracted with CH_2Cl_2 (20 mL), and the combined organic phase was evaporated to dryness under reduced pressure. The resulting residue was purified by silica gel column chromatography (0−35% EtOAc in toluene) to afford the desired phosphoramidites **4A**−**D** (512 mg, 73%) as white foams in three fractions containing phosphoramidites [**4A** and **4B**, 228 mg, 33%], [**4C** and **4D**, 130 mg, 17%], and [**4A**−**D**, 154 mg, 22%], respectively. Phosphoramidites **4A** and **4B** (1:4 ratio, based on ^{31}P NMR): TLC (50% EtOAc in PE) R_f = 0.55; ^{31}P NMR ($CDCl_3$) δ 149.5 (P_A), 150.1 (P_B) ppm; ESI-HiRes *m/z* 769.3008 ([M + Na]$^+$, $C_{39}H_{47}N_4O_9PNa^+$ calcd 769.2973). Phosphoramidites **4C** and **4D** (6:1 ratio, based on ^{31}P NMR): TLC (50% EtOAc in PE) R_f = 0.45; ^{31}P NMR ($CDCl_3$) δ 152.0 (P_C), 152.4 (P_D) ppm; ESI-HiRes *m/z* 769.2953 ([M + Na]$^+$, $C_{39}H_{47}N_4O_9PNa^+$ calcd 769.2973).

(2*R*/*S*,3*R*,5*R*)-3-(4,4′-Dimethoxytrityloxymethyl)-5-(uracil-1-yl)-1,4-dioxan-2-yl Hydrogen Phosphonate Triethylamine (5*R*/*S*). Anhydrous Et_3N (2.55 mL, 18.3 mmol) and imidazole (1.11 g, 16.4 mmol) were dissolved in anhydrous CH_3CN (25 mL), and the resulting mixture was cooled to 0 °C. PCl_3 (0.45 mL, 5.14 mmol) was added dropwise to the solution resulting in formation of a white precipitate. Hemiacetal **3** (399 mg, 0.729 mmol) was coevaporated with CH_3CN (5 mL) and redissolved in anhydrous CH_3CN (5 mL), and the resulting mixture was added dropwise to the above suspension under stirring at 0 °C. The reaction mixture was stirred for 22 h while the temperature was allowed to rise to rt, and then aq $Et_3NH{\cdot}HCO_3$ (2 M, 10 mL) was added. After being stirred for an additional 20 min, the reaction mixture was partitioned between CH_2Cl_2 (100 mL) and water (50 mL), and the organic phase was washed with satd aq $NaHCO_3$ (100 mL). The combined water phase was back-extracted with CH_2Cl_2 (100 mL), and the combined organic phase was evaporated to dryness under reduced pressure. The resulting residue was purified by silica gel column chromatography (0−10% MeOH in CH_2Cl_2, containing 1 vol % Et_3N) to afford an epimeric mixture of the desired *H*-phosphonates **5*R*/*S*** as a white foam (310 mg, 60%).

HPLC Separation of *H*-Phosphonates 5*R* and 5*S*. RP-HPLC separation of *H*-phosphonates **5*R*/*S*** was performed on 6−10 mg scale using a Waters Prep LC 4000 system equipped with an XBridge Prep C18, 5 μm, ODB (⌀ 19 mm × 100 mm). The gradient protocol used was an isocratic hold of 100% buffer A for 2 min, followed by a linear gradient to 30% buffer B over 5 min, and a linear gradient to 47% buffer B over 45 min at a flow rate of 8.0 mL/min (buffer A: 0.05 M aqueous triethylammonium acetate, pH = 7.4; buffer B: 75% acetonitrile in buffer A (v/v)). The protocol gave sufficient separation (t_R(5*R*) = 43.9 min, t_R(5*S*) = 45.8 min), and appropriate fractions were pooled, concentrated under reduced pressure, and then lyophilized affording the two epimers as white foams.

(2*R*,3*R*,5*R*)-3-(4,4′-Dimethoxytrityloxymethyl)-5-(uracil-1-yl)-1,4-dioxan-2-yl hydrogen phosphonate triethylamine (5*R*): ^{1}H NMR ($CDCl_3$) δ 7.62 (d with 6.02, 0.5H, PH, $J_{H,P}$ = 642), 7.61 (d, $J_{6,5}$ = 8.2, 1H, H6), 7.42−7.45 (m, 2H, $H2''_{DMT}$, $H6''_{DMT}$), 7.29−7.33 (m, 4H, $H2_{DMT}$, $H6_{DMT}$, $H2'_{DMT}$, $H6'_{DMT}$), 7.23−7.29 (m, 2H, $H3''_{DMT}$, $H5''_{DMT}$), 7.18−7.22 (m, 1H, $H4''_{DMT}$), 6.78−6.82 (m, 4H, $H3_{DMT}$, $H5_{DMT}$, $H3'_{DMT}$, $H5'_{DMT}$), 6.02 (d with 7.62, 0.5H, PH, $J_{H,P}$ = 642), 5.92 (dd, $J_{1',2'B}$ = 6.9, $J_{1',2'A}$ = 3.1, 1H, H1′), 5.74 (d, $J_{5,6}$ = 8.2, 1H, H5), 5.49 (dd, $J_{3',P}$ = 8.4, $J_{3',4'}$ = 7.9, 1H, H3′), 4.13 (dd, $J_{2'A,2'B}$ = 12.1, $J_{2'A,1'}$ = 3.1, 1H, $H2'_A$), 3.81−3.86 (m, 1H, H4′), 3.80 (s, 1H, *H*NEt_3), 3.78 (s, 6H, OCH_3), 3.64 (dd, $J_{2'B,2'A}$ = 12.1, $J_{2'B,1'}$ = 6.9, 1H, $H2'_B$), 3.40 ($m_{ABX,A}$, $J_{5'A,5'B}$ = 10.6, $J_{5'A,4'}$ = 2.2, 1H, $H5'_A$), 3.33 ($m_{ABX,B}$, $J_{5'B,5'A}$ = 10.6, $J_{5'B,4'}$ = 4.6, 1H, $H5'_B$), 3.01 (q, $J_{CH2,CH3}$ = 7.3, 6H, NCH_2), 1.28 (t, $J_{CH3,CH2}$ = 7.3, 9H, CH_2CH_3) ppm;[59] ^{13}C NMR ($CDCl_3$) δ 162.6 (C4), 158.5 ($C4_{DMT}$, $C4'_{DMT}$), 149.8 (C2), 144.6 ($C1''_{DMT}$), 139.9 (C6), 135.8 ($C1_{DMT}/C1'_{DMT}$), 135.7 ($C1_{DMT}/C1'_{DMT}$), 130.2 ($C2_{DMT}$, $C6_{DMT}$, $C2'_{DMT}$, $C6'_{DMT}$), 128.3 ($C2''_{DMT}$, $C6''_{DMT}$), 127.8 ($C3''_{DMT}$, $C5''_{DMT}$), 126.9 ($C4''_{DMT}$), 113.2 ($C3_{DMT}$, $C5_{DMT}/C3'_{DMT}$, $C5'_{DMT}$), 113.1 ($C3_{DMT}$, $C5_{DMT}/C3'_{DMT}$, $C5'_{DMT}$), 102.4 (C5), 92.4 (C3′), 86.2 (CAr_3), 78.6 (C1′), 77.2 (C4′), 64.7 (C2′), 62.1 (C5′), 55.2 (OCH_3), 45.5 (NCH_2), 8.6 (NCH_2CH_3) ppm; ^{31}P NMR ($CDCl_3$) δ 1.95 ppm; ESI-HiRes *m/z* 734.2783 ([M + Na]$^+$, $C_{36}H_{46}N_3O_{10}PNa^+$ calcd 734.2813).

(2*S*,3*R*,5*R*)-3-(4,4′-Dimethoxytrityloxymethyl)-5-(uracil-1-yl)-1,4-dioxan-2-yl hydrogen phosphonate triethylamine (5*S*): ^{1}H NMR ($CDCl_3$) δ 7.63 (d with 6.04, 0.5H, PH, $J_{H,P}$ = 636), 7.57 (d, $J_{6,5}$ = 8.2, 1H, H6), 7.40−7.44 (m, 2H, $H2''_{DMT}$, $H6''_{DMT}$), 7.28−7.32 (m, 4H, $H2_{DMT}$, $H6_{DMT}$, $H2'_{DMT}$, $H6'_{DMT}$), 7.23−7.28 (m, 2H, $H3''_{DMT}$, $H5''_{DMT}$), 7.17−7.21 (m, 1H, $H4''_{DMT}$), 6.77−6.82 (m, 4H, $H3_{DMT}$, $H5_{DMT}$, $H3'_{DMT}$, $H5'_{DMT}$), 6.04 (d with 7.63, 0.5H, PH, $J_{H,P}$ = 636), 5.89 ($dd_{ABX,X}$, $J_{1',2'A}$ = 10.2, $J_{1',2'B}$ = 3.2, 1H, H1′), 5.74 (d, $J_{5,6}$ = 8.2, 1H, H5), 5.39 (dd, $J_{3',P}$ = 8.2, $J_{3',4'}$ = 1.3, 1H, H3′), 4.06−4.13 (m, 1H, H4′), 3.93 ($dd_{ABX,A}$, $J_{2'A,2'B}$ = 11.2, $J_{2'A,1'}$ = 10.2, 1H, $H2'_A$), 3.80 (s, 1H, *H*NEt_3), 3.782 (s, 3H, OCH_3), 3.779 (s, 3H, OCH_3), 3.66 ($dd_{ABX,B}$, $J_{2'B,2'A}$ = 11.2, $J_{2'B,1'}$ = 3.2, 1H, $H2'_B$), 3.38 ($dd_{ABX,A}$, $J_{5'A,5'B}$ = 10.1, $J_{5'A,4'}$ = 6.8, 1H, $H5'_A$), 3.18 ($dd_{ABX,B}$, $J_{5'B,5'A}$ = 10.1, $J_{5'B,4'}$ = 4.8, 1H, $H5'_B$), 3.00 (q, $J_{CH2,CH3}$ = 7.3, 6H, NCH_2), 1.27 (t, $J_{CH3,CH2}$ = 7.3, 9H, CH_2CH_3) ppm;[60] ^{13}C NMR ($CDCl_3$) δ 162.5 (C4), 158.5 ($C4_{DMT}$, $C4'_{DMT}$), 149.6 (C2), 144.7 ($C1''_{DMT}$), 140.2 (C6), 136.0 ($C1_{DMT}/C1'_{DMT}$), 135.7 ($C1_{DMT}/C1'_{DMT}$), 130.2 ($C2_{DMT}$, $C6_{DMT}/C2'_{DMT}$, $C6'_{DMT}$), 130.1 ($C2_{DMT}$, $C6_{DMT}/C2'_{DMT}$, $C6'_{DMT}$), 128.2 ($C2''_{DMT}$, $C6''_{DMT}$), 127.8 ($C3''_{DMT}$, $C5''_{DMT}$), 126.8 ($C4''_{DMT}$), 113.2 ($C3_{DMT}$, $C5_{DMT}/C3'_{DMT}$, $C5'_{DMT}$), 113.1 ($C3_{DMT}$, $C5_{DMT}/C3'_{DMT}$, $C5'_{DMT}$), 102.5 (C5), 89.1 (C3′), 86.3 (CAr_3), 78.3 (C1′), 77.2 (C4′), 62.7 (C5′), 60.3 (C2′), 55.2 (OCH_3), 45.5 (NCH_2), 8.6 (CH_2CH_3) ppm; ^{31}P NMR ($CDCl_3$) δ 1.85 ppm; ESI-HiRes *m/z* 734.2786 ([M + Na]$^+$, $C_{36}H_{46}N_3O_{10}PNa^+$ calcd 734.2813).

Protocol for ON Synthesis. ONs were synthesized on 0.2 μmol or 1 μmol scale using succinyl-linked LCAA-CPG (long-chain alkylamine controlled pore glass, pore size 500 Å) DNA C columns. Coupling cycle: deblocking (3% trichloroacetic acid in dichloromethane, 1.0 mL over 1 min); wash A (CH_3CN, 2.0 mL over 1 min); neutralizer (CH_3CN/pyridine, 50:50, v/v, 1.0 mL over 1 min); coupling (premixing *H*-phosphonate (200 μL, 50 mM, in CH_3CN/pyridine, 50:50, v/v) and adamantane carbonyl chloride (200 μL, 200

dx.doi.org/10.1021/jo300222q | J. Org. Chem. 2012, 77, 3878−3886

mM, in CH_3CN/pyridine, 95:5, v/v), then adding over 2 min); wash B (CH_3CN/pyridine, 75:25, v/v, 1.0 mL over 1 min); coupling (as above); wash B (as above); wash A (as above). Oxidation after full-length ON synthesis: I_2, (78 mM in pyridine/water, 98:2, v/v, 20 mL over 30 min); wash A (as above).

After deprotection and cleavage from solid support (32% aq NH_3, 12 h, 55 °C), ONs were purified by RP-HPLC using a Waters 600 system equipped with an Xterra MS C18 (10 μm, 7.8 × 10 mm) precolumn and an Xterra MS C18 (10 μm, 7.8 × 150 mm) column using the representative gradient protocol depicted in Table S1 (Supporting Information), followed by detritylation (80% aq AcOH, 20 min, rt), precipitation (abs EtOH, −18 °C, 12−16 h) and washing (abs EtOH (2 × 300 μL)). The composition of the synthesized ONs was verified by MALDI-MS analysis (**ON2** (5′-GTG AXA TGC): $[M + H]^+$ *m/z* 2756 calcd 2755; **ON3** (5′-GTG AYA TGC) $[M + H]^+$ *m/z* 2753 calcd 2755) recorded in positive ion mode on a PerSeptive Voyager STR using 3-hydroxypicolinic acid as a matrix. The purity (>80%) was verified by ion-exchange HPLC using an a LaChrom L-7000 system equipped with a Dionex PA100 column (4 × 250 mm) at 80 °C and pH 8 using the representative protocol shown in Table S2 (Supporting Information).

■ ASSOCIATED CONTENT

Ⓢ Supporting Information

General experimental section, RP-HPLC profiles of phosphoramidites **4A/B**, RP-HPLC ON purification protocol (Table S1), IE-HPLC ON analytical protocol (Table S2), IE-HPLC profiles of ONs after 2 weeks, and copies of NMR spectra of compounds **2**−**5**. This material is available free of charge via the Internet at http://pubs.acs.org.

■ AUTHOR INFORMATION

Corresponding Author

*E-mail: jwe@sdu.dk.

Notes

The authors declare no competing financial interest.

■ ACKNOWLEDGMENTS

We greatly appreciate funding from The Danish National Research Foundation. We thank Ribotask ApS for assistance with HPLC purification and Dr. Michael Wamberg for assistance during oligonucleotide synthesis.

■ REFERENCES

(1) Leumann, C. J. *Bioorg. Med. Chem.* **2002**, *10*, 841−854.
(2) Herdewijn, P. *Chem. Biodivers.* **2010**, *7*, 1−59.
(3) Robin, A.; Julienne, K.; Meslin, J.-C.; Deniaud, D. *Eur. J. Org. Chem.* **2006**, *3*, 634−643.
(4) Barral, K.; Halfon, P.; Pèpe, G.; Camplo, M. *Tetrahedron Lett.* **2002**, *43*, 81−84.
(5) Barral, K.; Courcambeck, J.; Pèpe, G.; Balzarini, J.; Neyts, J.; De Clercq, E.; Camplo, M. *J. Med. Chem.* **2005**, *48*, 450−456.
(6) Vyas, D. M.; Szarek, W. A. *Carbohydr. Res.* **1973**, *30*, 225−227.
(7) Szarek, W. A.; Vyas, D. M.; Achmatowicz, B. *J. Heterocycl. Chem.* **1975**, *12*, 123−127.
(8) Hronowski, L. J. J.; Szarek, W. A. *J. Med. Chem.* **1982**, *25*, 522−526.
(9) Iwasaki, T.; Nishitani, T.; Horikawa, H.; Inoue, I. *Tetrahedron Lett.* **1981**, *22*, 1029−1032.
(10) Jones, A. S.; Walker, R. T.; Wyatt, P. G.; Balzarini, J.; De Clercq, E. *J. Chem. Res., Synop.* **1985**, 336−337.
(11) Prisbe, E. J. *J. Med. Chem.* **1986**, *29*, 2445−2450.
(12) Van Aerschot, A.; Janssen, G.; Herdewijn, P. *Bull. Soc. Chim. Belg.* **1990**, *99*, 769−777.
(13) Das, A. K.; Datta, M.; Mazumdar, S. K.; Das, N.; Van Aerschot, A.; Low, J. N.; Howie, R. A. *J. Cryst. Spectrosc. Res.* **1992**, *22*, 439−442.
(14) Maeda, M.; Kajimoto, N.; Yamaizumi, Z.; Okamoto, Y.; Nagahara, K.; Takayanagi, H. *Tetrahedron Lett.* **1997**, *38*, 6841−6844.
(15) Jones, A. S.; Markham, A. F.; Walker, R. T. *J. Chem. Soc., Perkin Trans. 1* **1976**, 1567−1570.
(16) Jones, A. S.; McClean, M. J.; Tanaka, H.; Walker, R. T.; Balzarini, J.; De Clercq, E. *Tetrahedron* **1985**, *41*, 5965−5972.
(17) Eschenmoser, A. *Science* **1999**, *284*, 2118−2124.
(18) Sabatino, D.; Damha, M. J. *J. Am. Chem. Soc.* **2007**, *129*, 8259−8270.
(19) Van Aerschot, A.; Verheggen, I.; Hendrix, C.; Herdewijn, P. *Angew. Chem., Int. Ed.* **1995**, *34*, 1338−1339.
(20) Hossain, N.; Wroblowski, B.; Van Aerschot, A.; Rozenski, J.; De Bruyn, A.; Herdewijn, P. *J. Org. Chem.* **1998**, *63*, 1574−1582.
(21) Allart, B.; Khan, K.; Rosemeyer, H.; Schepers, G.; Hendrix, C.; Rothenbacher, K.; Seela, F.; Van Aerschot, A.; Herdewijn, P. *Chem.—Eur. J.* **1999**, *5*, 2424−2431.
(22) Vandermeeren, M.; Préveral, S.; Janssens, S.; Geysen, J.; Saison-Behmoaras, E.; Van Aerschot, A.; Herdewijn, P. *Biochem. Pharmacol.* **2000**, *59*, 655−563.
(23) Maurinsh, Y.; Rosemeyer, H.; Esnouf, R.; Medvedovici, A.; Wang, J.; Ceulemans, G.; Lescrinier, E.; Hendrix, C.; Busson, R.; Sandra, P.; Seela, F.; Van Aerschot, A.; Herdewijn, P. *Chem.—Eur. J.* **1999**, *5*, 2139−2150.
(24) Wang, J.; Herdewijn, P. *J. Org. Chem.* **1999**, *64*, 7820−7827.
(25) Wang, J.; Verbeure, B.; Luyten, I.; Lescrinier, E.; Froeyen, M.; Hendrix, C.; Rosemeyer, H.; Seela, F.; Van Aerschot, A.; Herdewijn, P. *J. Am. Chem. Soc.* **2000**, *122*, 8595−8602.
(26) Summerton, J. *Biochim. Biophys. Acta, Gene Struct. Expression* **1999**, *1489*, 141−158.
(27) Since the synthetic strategy initiates from a ribofuranose the numeration throughout the manuscript follows standard nucleoside nomenclature (i.e., the nucleobase is attached to C1′, etc.)
(28) Altona, C.; Sundaralingam, M. *J. Am. Chem. Soc.* **1972**, *94*, 8205−8212.
(29) Olson, W. K.; Sussman, J. L. *J. Am. Chem. Soc.* **1982**, *104*, 270−278.
(30) Anet, F. A. L.; Sandstrom, J. *Chem. Commun.* **1971**, 1558−1559.
(31) Jensen, F. R.; Neese, R. A. *J. Am. Chem. Soc.* **1971**, *93*, 6329−6330.
(32) Chapman, D. M.; Hester, R. E. *J. Phys. Chem. A* **1997**, *101*, 3382−3387.
(33) Durig, J. R.; Zheng, C.; El Defrawy, A. M.; Ward, R. M.; Gounev, T. K.; Ravindranath, K.; Rajeswara Rao, N. *J. Raman Spectrosc.* **2009**, *40*, 197−204.
(34) Langkjær, N.; Pasternak, A.; Wengel, J. *Bioorg. Med. Chem.* **2009**, *17*, 5420−5425.
(35) More, J. D.; Finney, N. S. *Org. Lett.* **2002**, *4*, 3001−3003.
(36) Rohr, K.; Vogel, S. *ChemBioChem* **2006**, *7*, 463−470.
(37) Berner, S.; Mühlegger, K.; Seliger, H. *Nucleic Acids Res.* **1989**, *17*, 853−864.
(38) (a) Coppola, C.; Simeone, L.; De Napoli, L.; Montesarchio, D. *Eur. J. Org. Chem.* **2011**, *6*, 1155−1165. (b) Fujita, S.; Oka, N.; Wada, T. *J. Org. Chem.* **2011**, *76*, 2648.
(39) Sinha, N. D.; Biernat, J.; Köster, H. *Tetrahedron Lett.* **1983**, *24*, 5843−5846.
(40) Sinha, N. D.; Biernat, J.; McManus, J.; Köster, H. *Nucleic Acids Res.* **1984**, *12*, 4539−4557.
(41) Beaucage, S. L.; Iyer, R. P. *Tetrahedron* **1992**, *48*, 2223−2311.
(42) Beaucage, S. L.; Caruthers, M. H. In *Current Protocols in Nucleic Acid Chemistry*; Wiley: New York, 2000, p 3.3.1.
(43) (a) Reese, C. B. *Tetrahedron* **1978**, *34*, 3143−3179. (b) Itakura, K.; Bahl, C. P.; Katagiri, N.; Michniewicz, J.; Wightman, R. H.; Narang, S. A. *Can. J. Chem.* **1973**, *51*, 3469−3471. (c) Katagiri, N.; Itakura, K.; Narang, S. A. *J. Am. Chem. Soc.* **1975**, *97*, 7332−7337. (d) Garegg, P. J.; Lindh, I.; Regberg, T.; Stawinski, J.; Strömberg, R.; Henrichson, C. *Tetrahedron Lett.* **1986**, *27*, 4051−4054. (e) Garegg, P. J.; Lindh, I.; Regberg, T.; Stawinski, J.; Strömberg, R.; Henrichson, C. *Tetrahedron Lett.* **1986**, *27*, 4055−4058. (f) Froehler, B. C.; Matteucci, M. D.

Tetrahedron Lett. **1986**, *27*, 469−472. (g) Froehler, B. C.; Ng, P. G.; Matteucci, M. D. *Nucleic Acids Res.* **1986**, *14*, 5399−5407.
(44) Stawinski, J.; Kraszewski, A. *Acc. Chem. Res.* **2002**, *35*, 952−960.
(45) Berkin, A.; Coxon, B.; Pozsgay, V. *Chem.—Eur. J.* **2002**, *8*, 4424−4433.
(46) Ruhela, D.; Vishwakarma, R. A. *J. Org. Chem.* **2003**, *68*, 4446−4456.
(47) Slättegard, R.; Teodorovic, P.; Kinfe, H. H.; Ravenscroft, N.; Gammon, D. W.; Oscarson, S. *Org. Biomol. Chem.* **2005**, *3*, 3782−3787.
(48) Donahue, M. G.; Johnston, J. N. *Bioorg. Med. Chem. Lett.* **2006**, *16*, 5602−5604.
(49) Díez, E.; San-Fabián, J.; Guilleme, J.; Altona, C.; Donders, L. A. *Mol. Phys.* **1989**, *68*, 49−63.
(50) Navarro-Vázquez, A.; Cobas, J. C.; Sardina, F. J.; Casanueva, J.; Díez, E. *J. Chem. Inf. Comput. Sci.* **2004**, *44*, 1680−1685.
(51) MacroModel, version 9.8, Schrödinger, LLC, New York, 2010.
(52) Cornell, W. D.; Cieplak, P.; Bayly, C. I.; Gould, I. R.; Merz, K. M.; Ferguson, D. M.; Spellmeyer, D. C.; Fox, T.; Caldwell, J. W.; Kollman, P. A. *J. Am. Chem. Soc.* **1995**, *117*, 5179−5197.
(53) Pérez, A.; Marchán, I.; Svozil, D.; Sponer, J.; Cheatham, T. E.; Laughton, C. A.; Orozco, M. *Biophys. J.* **2007**, *92*, 3817−3829.
(54) Still, W. C.; Tempczyk, A.; Hawley, R. C.; Hendrickson, T. *J. Am. Chem. Soc.* **1990**, *112*, 6127−6129.
(55) Petersen, M.; Nielsen, C. B.; Nielsen, K. E.; Jensen, G. A.; Bondensgaard, K.; Singh, S. K.; Rajwanshi, V. K.; Koshkin, A. A.; Dahl, B. M.; Wengel, J.; Jacobsen, J. P. *J. Mol. Recognit.* **2000**, *13*, 44−53.
(56) Nielsen, C. B.; Singh, S. K.; Wengel, J.; Jacobsen, J. P. *J. Biomol. Struct. Dyn.* **1999**, *17*, 175−191.
(57) Nielsen, K. E.; Singh, S. K.; Wengel, J.; Jacobsen, J. P. *Bioconjugate Chem.* **2000**, *11*, 228−238.
(58) As integrals of the hemiacetals were in a 1:1 ratio, the integrals of resolved signals (corresponding to one proton) have been set to 1H and accordingly overlapping signals (corresponding to one proton) have integrals of 2H.
(59) The HP signal is at 6.82 (d, $J_{H,P}$ = 642, 1H, HP) but is given here as separate peaks because of the large coupling constant.
(60) The HP signal is at 6.84 (d, $J_{H,P}$ = 636, 1H, HP) but is given here as separate peaks because of the large coupling constant.